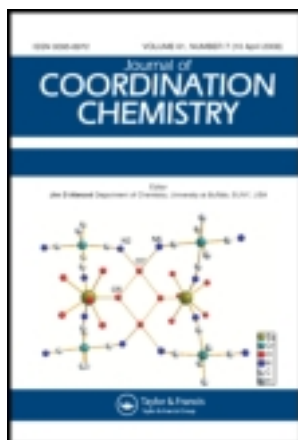


This article was downloaded by: [Renmin University of China]

On: 13 October 2013, At: 10:25

Publisher: Taylor & Francis

Informa Ltd Registered in England and Wales Registered Number: 1072954 Registered office: Mortimer House, 37-41 Mortimer Street, London W1T 3JH, UK



Journal of Coordination Chemistry

Publication details, including instructions for authors and subscription information:

<http://www.tandfonline.com/loi/gcoo20>

Two new coordination polymers constructed by angular tripyridyl ligand: syntheses, structures, and properties

Lian Wu^a, Ya-Hui Yu^a, Xiao-Ju Yuan^a, Cai-Qin Chu^a, Ben-Lai Wu^a & Hong-Yun Zhang^a

^a Department of Chemistry, Zhengzhou University, Zhengzhou 450052, P.R. China

Published online: 12 Aug 2011.

To cite this article: Lian Wu, Ya-Hui Yu, Xiao-Ju Yuan, Cai-Qin Chu, Ben-Lai Wu & Hong-Yun Zhang (2011) Two new coordination polymers constructed by angular tripyridyl ligand: syntheses, structures, and properties, *Journal of Coordination Chemistry*, 64:16, 2804-2814, DOI: [10.1080/00958972.2011.607494](https://doi.org/10.1080/00958972.2011.607494)

To link to this article: <http://dx.doi.org/10.1080/00958972.2011.607494>

PLEASE SCROLL DOWN FOR ARTICLE

Taylor & Francis makes every effort to ensure the accuracy of all the information (the "Content") contained in the publications on our platform. However, Taylor & Francis, our agents, and our licensors make no representations or warranties whatsoever as to the accuracy, completeness, or suitability for any purpose of the Content. Any opinions and views expressed in this publication are the opinions and views of the authors, and are not the views of or endorsed by Taylor & Francis. The accuracy of the Content should not be relied upon and should be independently verified with primary sources of information. Taylor and Francis shall not be liable for any losses, actions, claims, proceedings, demands, costs, expenses, damages, and other liabilities whatsoever or howsoever caused arising directly or indirectly in connection with, in relation to or arising out of the use of the Content.

This article may be used for research, teaching, and private study purposes. Any substantial or systematic reproduction, redistribution, reselling, loan, sub-licensing, systematic supply, or distribution in any form to anyone is expressly forbidden. Terms &

Conditions of access and use can be found at <http://www.tandfonline.com/page/terms-and-conditions>

Two new coordination polymers constructed by angular tripyridyl ligand: syntheses, structures, and properties

LIAN WU, YA-HUI YU, XIAO-JU YUAN, CAI-QIN CHU,
BEN-LAI WU* and HONG-YUN ZHANG

Department of Chemistry, Zhengzhou University, Zhengzhou 450052, P.R. China

(Received 27 April 2011; in final form 30 June 2011)

U-shaped tripyridyl ligand 2,6-bis(pyridine-4-carboxamido)pyridine (L) was synthesized and used to assemble metal complexes. The resulting new complexes $[\text{Mn}(\text{L})_3(\text{SCN})_2]_n$ (**1**) and $[\text{Co}(\text{L})_3(\text{SCN})_2]_n$ (**2**) are isostructural, crystallizing in the monoclinic $C2/c$ space group. In compounds **1** and **2**, each metal is in a slightly distorted octahedron ligated by six nitrogens from four L and two SCN^- . Complexes **1** and **2** possess infinite 1-D zigzag polymeric chain structures where L adopts bridge and terminal coordination. These 1-D coordination polymers assemble into 3-D supermolecules of compounds **1** and **2** through hydrogen bonds. Fluorescence measurements and thermal analysis show that **1** emits strong fluorescence with a single broad band centered at 410 nm upon excitation at 357 nm and the polymeric chain structure is stable up to 340°C.

Keywords: Angular tripyridyl ligand; Crystal structure; Coordination polymer; Fluorescent property

1. Introduction

Metal–organic architectures have drawn great interest in supermolecular and material chemistry [1, 2], driven by the intriguing architectures [3–6] and promising applications in magnetism, electric conductivity, ion exchange, separation, molecular adsorption, heterogeneous catalysis [7–17], and fluorescent materials [18–25].

Pyridylcarboxamides have an important position in biochemistry and coordination chemistry [26]. Especially, polytopic pyridinecarboxamide ligands combining rigidity and flexibility were designed to synthesize well-defined functional architectures such as metal-containing macrocycles, nanocages, and intriguing metal–organic frameworks [27, 28]. Apart from their coordination ability, such spacers are endowed with other special merits such as various conformations (sometimes displaying a dominant conformer), potential helicity, and rich hydrogen-bonding sites which can be used to direct self-assembly with metal ions. For example, assembly of U-shaped ligands 1,2-bis(3-pyridylcarboxylamide)benzene and 1,2-bis(4-pyridylcarboxylamide)benzene with d^{10} metal ions Ag(I), Au(I), and Hg(II) as well as Cu(II) resulted in macrocyclic or

*Corresponding author. Email: wbl@zzu.edu.cn

polymeric complexes; the metal-containing arrays can be further organized by hydrogen bonds between amide substituents in the well-known patterns of the free *bis*(amidopyridine) ligands [29, 30]. Our group used achiral N^2, N^6 -*bis*((pyridin-2-yl)methyl)pyridine-2,6-dicarboxamide to react with $AgAsF_6$ and $AgSbF_6$, obtaining two enantiomeric 3-D chiral architectures with unusual (10,3) nets where the helical conformer of the ligand is fixed in the resulting chiral 1-D coordination polymers with helical chirality expanding along the chain [31].

Herein, we synthesized the symmetric U-shaped bispyridylcarboxamide ligand 2,6-*bis*(pyridine-4-carboxamido)pyridine (L). As shown in scheme 1, L is a multifunctional bridge with two isonicotinamide pendants symmetrically bonding at sites 2 and 6 of the central pyridine. The structure L is a promising one and we obtain metal-organic architectures. Self-assembly of L with Mn(II) and Co(II) resulted in $[Mn(L)_3(SCN)_2]_n$ (**1**) and $[Co(L)_3(SCN)_2]_n$ (**2**), where 1-D coordination polymer chains assemble into 3-D supermolecules through hydrogen bonds.

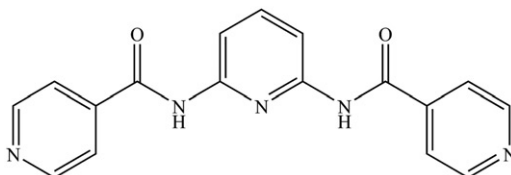
2. Experimental

2.1. General information and materials

In this study, 2,6-Diaminopyridine was purchased from Alfa Aesar and used as received. Other chemicals were commercially available and used without purification. Some reagents used in ligand preparation, such as pyridine and thionyl chloride, were dried to remove water. IR data were recorded on a Nicolet IR-470 spectrophotometer with KBr pellets from 400 to 4000 cm^{-1} . Elemental analyses were performed with a Carlo-Erba 1106 elemental analyzer. The fluorescence spectrum was determined in the solid state at room temperature on a Hitachi F-4500 fluorophotometer with excitation and emission slits 5 nm and response time 1 s. Thermal analyses were scanned from 30°C to 700°C in air on a STA 409 PC thermal analyzer.

2.2. Syntheses

2.2.1. Synthesis of 2,6-*bis*(pyridine-4-carboxamido)pyridine (L). A mixture of isonicotinic acid (2.5 g, 20 mmol) and thionyl chloride (25 mL) was heated to reflux for 6 h under anhydrous conditions, and then excess thionyl chloride was removed by rotary evaporation. The resulting yellowish isonicotinoyl chloride solid was dissolved in anhydrous pyridine (15 mL), to which a solution of pyridine-2,6-diamine (1.1 g,



Scheme 1. Schematic representation of L.

10 mmol) and anhydrous pyridine (20 mL) was added dropwise with continuous stirring. After addition, the mixture was stirred at room temperature for 5 h. The resulting white precipitate was filtered, washed with water and methanol, and recrystallized from anhydrous ethanol, giving white crystals of pure **L** (2.3 g; yield: 73%). Elemental analysis Calcd (%) for $C_{17}H_{13}N_5O_2$: C, 63.94; H, 4.10; and N, 21.93. Found: C, 63.52; H, 4.13; and N, 21.73. Selected IR (KBr, cm^{-1}): 3434(m), 1690(vs), 1591(s), 1557(s), 1518(s), 1490(s), 1448(s), 1310(s), 1243(s), 1153(m), 1128(m), 1065(m), 895(m), 907(m), 805(m), 751(m), and 700(m).

2.2.2. Synthesis of $[Mn(L)_3(SCN)_2]_n$ (1**).** An ethanol solution (10 mL) of **L** (31.9 mg, 0.1 mmol) was added dropwise into 10 mL methanol solution of $MnCl_2 \cdot 4H_2O$ (19.89 mg, 0.1 mmol). To the resulting pale yellow solution, 5 mL methanol solution of KSCN was added dropwise (19.4 mg, 0.2 mmol), and then the mixture was stirred for 10 min. After filtration, the filtrate was allowed undisturbed evaporation at ambient temperature. One week later, pale yellow prismatic crystals of **1** suitable for X-ray single crystal diffraction were collected (Yield: 45%). Elemental analysis Calcd (%) for $C_{53}H_{39}N_{17}O_6S_2Mn_1$: C, 56.38; H, 3.48; N, 21.09; and S, 5.68. Found: C, 56.03; H, 3.52; N, 21.23; and S, 5.60. Selected IR (KBr, cm^{-1}): 3416(m), 3247(m), 2046(s), 1679(s), 1588(s), 1518(s), 1448(s), 1317(s), 1262(s), 1241(s), 1156(s), 1063(m), 808(m), and 704(m).

2.2.3. Synthesis of $[Co(L)_3(SCN)_2]_n$ (2**).** A DMF solution (5 mL) of **L** (31.9 mg, 0.1 mmol) was added dropwise into 10 mL methanol solution of $CoSO_4 \cdot 7H_2O$ (28 mg, 0.1 mmol). To the resulting purple solution, 5 mL methanol solution of KSCN was added dropwise (19.4 mg, 0.2 mmol), and then the mixture was stirred for 30 min. After filtration, the filtrate was allowed to undergo undisturbed evaporation at ambient temperature. One month later, dark red prismatic crystals of **2** suitable for X-ray single-crystal diffraction were obtained (Yield: 34%). Elemental analysis Calcd (%) for $C_{53}H_{39}N_{17}O_6S_2Co$: C, 56.18; H, 3.47; N, 21.02; and S, 5.66. Found: C, 56.41; H, 3.43; N, 20.87; and S, 5.73. Selected IR (KBr, cm^{-1}): 3414(m), 3240(m), 2057(s), 1680(s), 1587(s), 1519(s), 1316(s), 1240(s), 1098(m), 806(m), 751(m), 705(m), and 611(m).

2.3. Single-crystal structure determination

Single-crystal data of **1** and **2** were collected on a Bruker SMART APEXII CCD single-crystal diffractometer using Mo- $K\alpha$ radiation ($\lambda = 0.71073 \text{ \AA}$) at 293(2) K. Absorption corrections were performed using SADABS. Both structures were solved by direct methods and refined with full-matrix least-squares on F^2 using the SHELXTL program package [32]. All non-hydrogen atoms were refined anisotropically. Hydrogens in pyridyls were assigned with common isotropic displacement factors, while the hydrogens on the nitrogen of carboxylamide groups were located from difference Fourier maps and were constrained to ride on their parent atoms. Crystal data are summarized in detail in table 1. Selected bond lengths and angles are listed in tables 2 and 3.

Table 1. Crystal data and structure refinement for **1** and **2**.

	1	2
Empirical formula	C ₅₃ H ₄₃ N ₁₇ O ₆ S ₂ Mn	C ₅₃ H ₃₉ N ₁₇ O ₆ S ₂ Co
Formula weight	1133.10	1133.06
Temperature (K)	293(2)	293(2)
Crystal system	Monoclinic	Monoclinic
Space group	C2/c	C2/c
Crystal size (mm ³)	0.219 × 0.18 × 0.137	0.287 × 0.187 × 0.107
Unit cell dimensions (Å, °)		
<i>a</i>	19.745(4)	19.619(4)
<i>b</i>	21.497(4)	21.361(4)
<i>c</i>	15.445(3)	15.321(3)
α	90	90
β	127.23(3)	126.53(3)
γ	90	90
Volume (Å ³), <i>Z</i>	5219.7(18), 4	5159.4(17), 4
Calculated density (Mg m ⁻³)	1.437	1.459
Goodness-of-fit on <i>F</i> ²	1.022	1.052
Final <i>R</i> indices [<i>I</i> > 2σ(<i>I</i>)]	<i>R</i> ₁ = 0.0433, <i>wR</i> ₂ = 0.0934	<i>R</i> ₁ = 0.0445, <i>wR</i> ₂ = 0.0909
Largest difference peak and hole (e Å ⁻³)	0.440 and -0.400	0.405 and -0.402

Table 2. Selected bond lengths (Å) and angles (°) for **1** and **2**.

1 ^a			
Mn1–N1	2.150(3)	Mn1–N1A	2.150(3)
Mn1–N2	2.321(2)	Mn1–N2A	2.321(2)
Mn1–N7	2.321(2)	Mn1–N7A	2.321(2)
N1–Mn1–N1A	180.0	N1A–Mn1–N2A	90.57(9)
N1–Mn1–N2A	89.43(9)	N1A–Mn1–N2	89.43(9)
N1–Mn1–N2	90.57(9)	N2–Mn1–N2A	180.0
N1A–Mn1–N7	90.84(9)	N1–Mn1–N7	89.16(9)
N2A–Mn1–N7	83.83(8)	N2–Mn1–N7	96.17(8)
N1A–Mn1–N7A	89.16(9)	N1–Mn1–N7A	90.84(9)
N2A–Mn1–N7A	96.17(8)	N2–Mn1–N7A	83.83(8)
N7–Mn1–N7A	180.0		
2 ^b			
Co1–N1	2.060(3)	Co1–N1A	2.060(3)
Co1–N2	2.213(2)	Co1–N2A	2.213(2)
Co1–N7	2.221(2)	Co1–N7A	2.221(2)
N1A–Co1–N1	180.00(19)	N1A–Co1–N2	89.95(10)
N1–Co1–N2	90.05(10)	N1A–Co1–N2A	90.05(10)
N1–Co1–N2A	89.95(10)	N2A–Co1–N2	180.00(8)
N1A–Co1–N7A	91.09(9)	N1–Co1–N7A	88.91(9)
N2–Co1–N7A	96.35(9)	N2A–Co1–N7A	83.65(9)
N1A–Co1–N7	88.91(9)	N1–Co1–N7	91.09(9)
N2–Co1–N7	83.65(9)	N2A–Co1–N7	96.35(9)
N7A–Co1–N7	180.00(14)		

^aA: -*x* + 3/2, -*y* + 1/2, and -*z* + 2.^bA: -*x* + 3/2, -*y* + 1/2, and -*z*.

3. Results and discussion

3.1. IR spectra

For **L**, characteristic peaks for vibrations of N–H, C=O, and C–N bonds in amides appear at 3434, 1690, and 1518 cm⁻¹. IR spectra of **1** and **2** are similar. The strong and

Table 3. Hydrogen bonds of **1** and **2**.

D-H...A	<i>d</i> (D-H) (Å)	<i>d</i> (H...A) (Å)	<i>d</i> (D...H) (Å)	∠(D-H...A) (°)
1 ^a				
N8-H8...O2C	0.82(3)	2.08(3)	2.903(3)	175(3)
2 ^b				
N8-H8...O2C	0.95(0)	1.94(0)	2.888(3)	173.4(0)
N3-H3...N6D	1.05(0)	2.07(0)	3.107(4)	168.6(0)

^aC: $-x+2$, $-y+1$, $-z+2$.^bC: $x+1/2$, $y-1/2$, z ; D: $-x+3/2$, $-y+3/2$, and $-z$.

broad absorptions at 3100–3400 cm⁻¹ indicate the presence of –NH. Strong absorptions at 1518 and 1680 cm⁻¹ for **1** and **2** correspond to the C–N and C=O stretches in amide. In comparison with those of **L**, the absorptions of N–H, C–N, and C=O of amide in **1** and **2** slightly shift. Strong bands at 2046 and 2057 cm⁻¹ in IR spectra of **1** and **2** indicate the existence of SCN⁻. IR spectra of **1** and **2** are consistent with the single-crystal X-ray diffraction analyses.

3.2. Crystal structures of **1** and **2**

Complexes **1** and **2** crystallize in the monoclinic *C2/c* space group. They are isostructural and the structure of [Mn(L)₃(SCN)₂]_{*n*} is described herein representatively. In **1**, every Mn(II) located at the inversion center reproduces the whole molecule through the asymmetric unit consisting of one-half Mn(II), one and a half L, and one SCN⁻. As shown in figure 1, each Mn(II) is a slightly distorted octahedron ligated by four N atoms from four ligands L and two N atoms from two SCN⁻. In the equatorial plane, the four 4-pyridyl rings from four L arrays around Mn(II) in the well-known paddlewheel pattern with the in-plane angles being 180° and Mn–N bond lengths being 2.321(2) Å [33]; the two SCN⁻ located at the axial sites are almost perpendicular to the equatorial plane with N_{axial}–Mn–N_{equatorial} angles being very close to 90° and N_{axial}–Mn–N_{axial} angle being 180°. Mn–N bond lengths are 2.150(3) Å. The Mn–N_{equatorial} bond lengths are longer than Mn–N_{axial} and that of 2.277(3) Å in the literature [34].

The overall structure of **1** is an infinite 1-D zigzag chain presented in figure 2. Ligands L in **1** use nitrogens from 4-pyridyl of isonicotinamido groups to coordinate with Mn(II) in two coordination modes; one-third are bidentate bridging and the others terminal. The Mn(II)···Mn(II) distance by bridging L is 15.792 Å. The bidentate bridging L have C₂ symmetry with the two-fold axis passing through the nitrogen of central pyridyl of the Ligands L and the dihedral angle between 4-pyridyls of isonicotinamido groups is 78.1°, while terminal ligands L have C₁ or pseudo C₂ symmetry with the dihedral angle between 4-pyridyls of isonicotinamido groups being 46.5°.

In **1**, there are hydrogen-bonding interactions occurring between adjacent chains, which direct the assembly of chain structures. Figure 2 shows the hydrogen-bonding interactions between two adjacent chains arising from one NH of isonicotinamido of bridging L in one chain to the carbonyl oxygen of terminal Ligands L in the other [N8...O2=2.903(3) Å]. By this double hydrogen-bonding interaction, two adjacent chains wind together. This linkage between the two adjacent chains is stabilized through

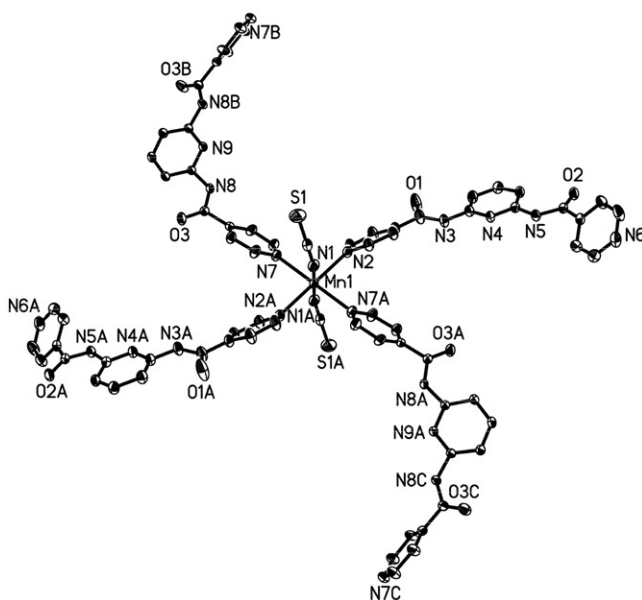


Figure 1. View of the coordination sphere around Mn(II) in **1** (hydrogens are omitted for clarity).

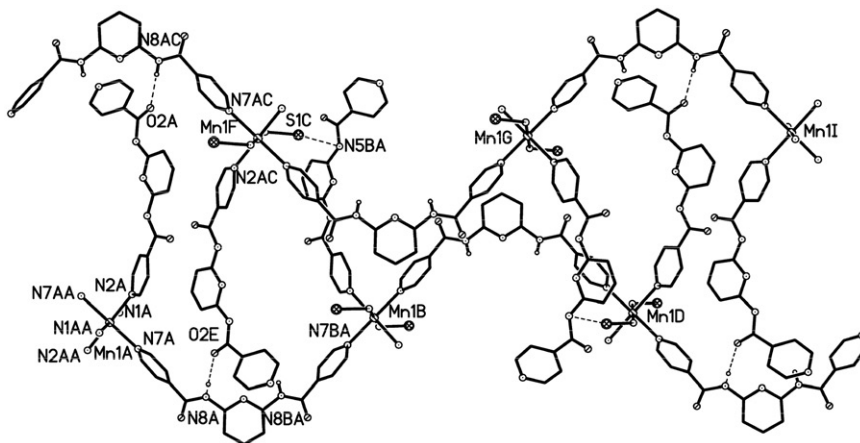


Figure 2. View of the two adjacent polymeric chains winding together through double hydrogen-bonding interactions of N–H...O in **1**.

weak interactions between S of SCN^- and N of terminal Ligands L from the adjacent chains ($\text{S1} \cdots \text{N} = 3.313 \text{ \AA}$) and $\pi \cdots \pi$ interactions between terminal L's with a mean distance from edge-to-centroid of 3.612 \AA . Through the double hydrogen-bonding interactions, every chain links with four adjacent chains (figure 3), and thus results in the formation of a 3-D supramolecular architecture. The isostructural 1-D polymeric chains in **2** display not only the hydrogen-bonding interaction pattern in **1** but also a new hydrogen-bonding connection, as shown in figure 4. Through double hydrogen-

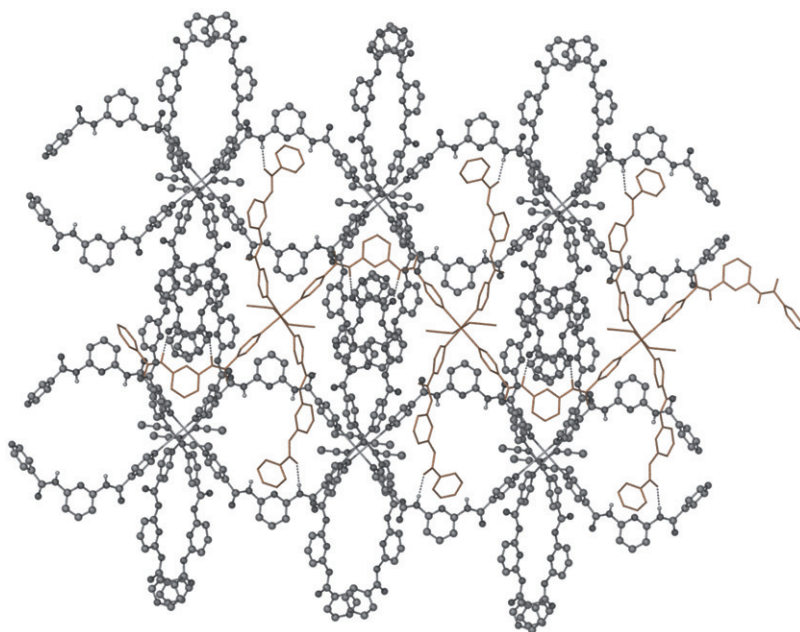


Figure 3. Representation of linkage through N–H···O hydrogen-bonding interactions in **1**, showing the polymeric chain drawn in stick bridges with four adjacent chains drawn in ball-and-stick representation.

bonding interactions between N3 and N6 from terminal ligands L of different chains [$N3 \cdots N6 = 3.107(4) \text{ \AA}$], each chain in **2** further bridges with two other chains. Consequently, every 1-D polymeric chain in **2** connects with six adjacent chains through hydrogen-bonding interactions (figure 5) to form a 3-D supramolecular architecture.

3.3. Thermal stability analysis

The DSC-TG curve of **1** (figure 6) was scanned from 30°C to 700°C on a STA 409 PC thermal analyzer under air with a flow rate of 30 mL min^{-1} and a heating rate of $10^\circ\text{C min}^{-1}$. At 340°C, a sharp weight loss was observed from 340°C and 464°C with a broad endothermic peak centered at 457°C and a weight loss of 54.1%, indicating the framework decomposition of **1**, and perhaps corresponds to partial loss of isonicotinamido groups of L. Successive mass loss of 34.31% at 464–640°C was accompanied with a sharp exothermic peak at 576°C, indicating complete decomposition of **1**. The remaining 11.6% may be Mn_2O_3 (Calcd 7.0%) and unburned carbon. Compound **1** is stable at 340°C, ascribed to coordination bonds and complicated hydrogen-bonding interactions.

3.4. Photoluminescence properties

The solid-state photoluminescence of L and **1** are investigated at room temperature (figure 7). Free L is photoluminescent. When excited at $\lambda_{\text{max}} = 380 \text{ nm}$, it exhibits

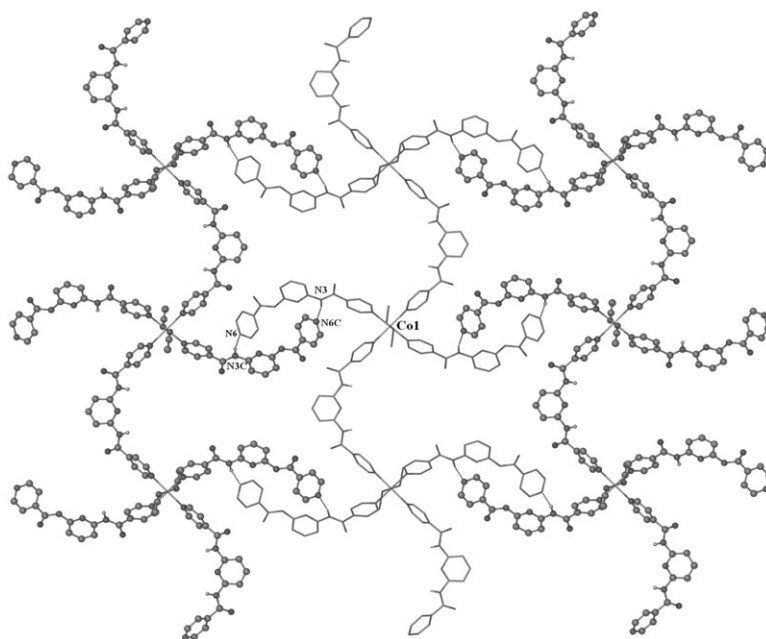


Figure 4. View of typical N-H...N hydrogen bonds in **2**.

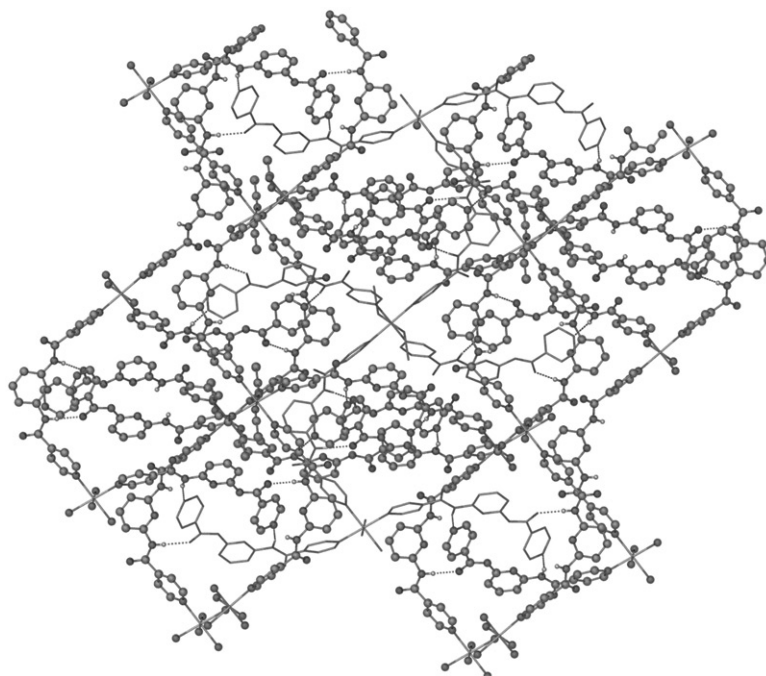
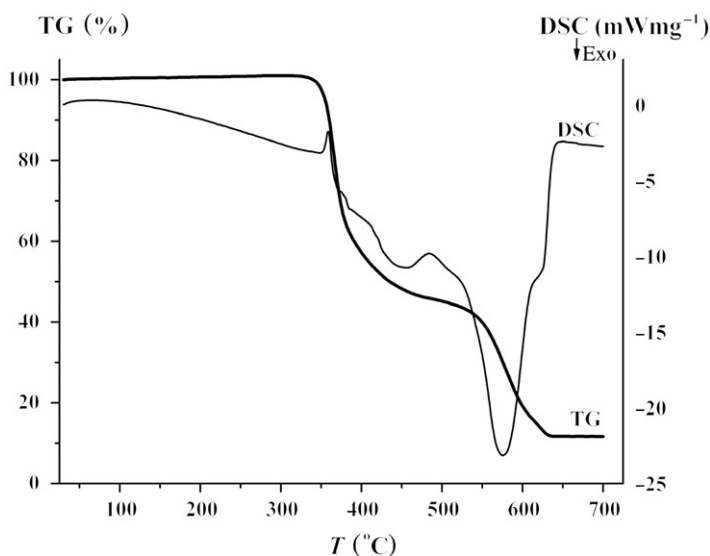
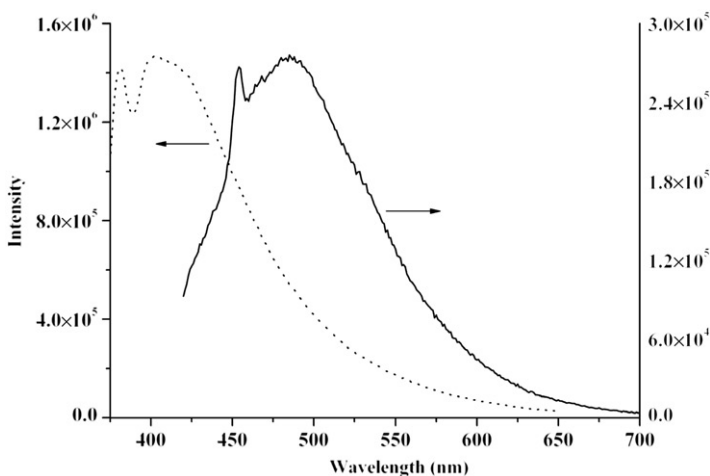


Figure 5. View of hydrogen-bonding connections in **2**, showing the polymeric chain drawn in stick binds with six adjacent chains drawn in ball-and-stick form through types of hydrogen-bonding interactions.

Figure 6. DSC-TG curve of **1**.Figure 7. Solid-state photoluminescent spectra of free **L** (solid line) and **1** (dotted line).

intense emission with a single broad band centered at 485 nm and a sharp weak scattering peak at 454 nm. Complex **1** displays strong emission with a single broad band centered at 410 nm and a sharp weak scattering peak at 380 nm upon excitation at 357 nm. In comparison with **L**'s fluorescence, the emission wavelength of **1** is blue-shifted by 75 nm and its intensity increased by about five times. The emission of **1** is mainly due to a ligand-centered emission state including significant charge transfer character induced by the polar Mn(II). In **1**, formation of coordination polymer chains as well as hydrogen-bonding connections and $\pi \cdots \pi$ interactions between chains

increase the rigidity of L, thereby reducing the non-radiative decay to enhance intraligand fluorescence. This contrasts with the weak emission of our recently reported dinuclear Mn(II) complex of a new polydentate double Schiff-base ligand derived from 1,10-phenanthroline [35].

4. Conclusions

Two new coordination compounds, $[\text{Mn}(\text{L})_3(\text{SCN})_2]_n$ (**1**) and $[\text{Co}(\text{L})_3(\text{SCN})_2]_n$ (**2**), have been obtained through reactions of Mn(II) and Co(II) salts with U-shaped tripyridyl ligand, 2,6-bis(pyridine-4-carboxamido)pyridine (L). Complexes **1** and **2** are isostructural and possess infinite 1-D zigzag polymeric chain structures where ligands L are bridging and terminal. These 1-D coordination polymer chains assemble into 3-D supermolecules of **1** and **2** through hydrogen bonds. Complex **1** is stable and can emit intense purple fluorescence centered at 410 nm. This study shows that multifunctional ligands L have excellent performance in supermolecular chemistry, and further construction of metal-organic complexes with intriguing architectures is underway in our laboratory.

References

- [1] M.A. Withersby, A.J. Blake, N.R. Champness, P. Hubberstey, W.S. Li, M. Schröder. *Angew. Chem. Int. Ed.*, **39**, 2327 (1997).
- [2] S.R. Batten, R. Robson. *Angew. Chem. Int. Ed.*, **37**, 1460 (1998).
- [3] J.W. Cheng, S.T. Zheng, E. Ma, G.Y. Yang. *Inorg. Chem.*, **46**, 10534 (2007).
- [4] M.C. Hong. *Cryst. Growth Des.*, **1**, 10 (2007).
- [5] B. Zhao, P. Cheng, X.Y. Chen, C. Cheng, W. Shi, D.Z. Liao, S.P. Yan, Z.H. Jiang. *J. Am. Chem. Soc.*, **126**, 3012 (2004).
- [6] M.S. Wickleder. *Chem. Rev.*, **102**, 2011 (2002).
- [7] R. Matsuda, R. Kitaura, S. Kitagawa, Y. Kubota, R.V. Belosludov, T.C. Kobayashi, H. Sakamoto, T. Chiba, M. Takata, Y. Kawazoe, Y. Mita. *Nature*, **436**, 238 (2005).
- [8] R. Matsuda, R. Kitaura, S. Kitagawa, Y. Kubota, T.C. Kobayashi, S. Horike, M. Takata. *J. Am. Chem. Soc.*, **126**, 14063 (2004).
- [9] S. Kitagawa, R. Kitaura, S. Noro. *Angew. Chem. Int. Ed.*, **43**, 2334 (2004).
- [10] O.M. Yaghi, M. O'Keeffe, N.W. Ockwing, H.K. Chae, M. Eddaoudi, J. Kim. *Nature*, **423**, 705 (2003).
- [11] C. Janiak. *J. Chem. Soc., Dalton Trans.*, 2781 (2003).
- [12] O.R. Evans, W. Lin. *Acc. Chem. Res.*, **35**, 511 (2002).
- [13] M. Eddaoudi, D.B. Moler, H. Li, B.L. Chen, T. Reineke, M. O'Keeffe, O.M. Yaghi. *Acc. Chem. Res.*, **34**, 319 (2001).
- [14] B.L. Chen, S.Q. Ma, F. Zapata, E.B. Lobkovsky, J. Yang. *Inorg. Chem.*, **45**, 5718 (2006).
- [15] B.L. Chen, S.Q. Ma, F. Zapata, F.R. Fronczek, E.B. Lobkovsky, H.C. Zhou. *Inorg. Chem.*, **46**, 1233 (2007).
- [16] S.R. Batten, K.S. Murray. *Coord. Chem. Rev.*, **246**, 103 (2003).
- [17] L. Carlucci, G. Ciani, D.M. Proserpio. *Coord. Chem. Rev.*, **246**, 247 (2003).
- [18] R.B. Fu, S.C. Xiang, S.M. Hu, L.S. Wang, Y.M. Li, X.H. Huang, X.T. Wu. *Chem. Commun.*, 5292 (2005).
- [19] J.C. Dai, X.T. Wu, S.M. Hu, Z.Y. Fu, J.J. Zhang, W.X. Du, H.H. Zhang, R.Q. Sun. *Eur. J. Inorg. Chem.*, 2096 (2004).
- [20] Q.R. Fang, G.S. Zhu, X. Shi, G. Wu, G. Tian, R.W. Wang, S.L. Qiu. *J. Solid State Chem.*, **177**, 1060 (2004).
- [21] M.L. Tong, X.M. Chen, B.H. Ye, L.N. Ji. *Angew. Chem. Int. Ed.*, **38**, 2237 (1999).
- [22] J. Zhang, Z.J. Li, Y. Kang, J.K. Cheng, Y.G. Yao. *Inorg. Chem.*, **43**, 8085 (2004).
- [23] Z.Y. Fu, X.T. Wu, J.C. Dai, L.M. Wu, C.P. Cui, S.M. Hu. *Chem. Commun.*, 1856 (2001).

- [24] X.P. Yang, B.P. Hahn, R.A. Jones, K.J. Stevenson, J.S. Swinnea, Q.Y. Wu. *Chem. Commun.*, 3827 (2006).
- [25] B.L. Chen, Y. Yang, F. Zapata, G.D. Qian, Y.S. Luo, J.H. Zhang, E.B. Lobkovsky. *Inorg. Chem.*, **45**, 8882 (2006).
- [26] (a) Z. He, C. He, Z.M. Wang, E.Q. Gao, Y. Liu, C.H. Yan. *Dalton Trans.*, 502 (2004); (b) D.S. Marlin, M.M. Olmstead, P.K. Mascharak. *Eur. J. Inorg. Chem.*, 859 (2002).
- [27] (a) T.J. Burchell, D.J. Eisler, R.J. Puddephatt. *Cryst. Growth Des.*, **6**, 974 (2006); (b) J. Pansanel, A. Jouaiti, S. Ferlay, M.W. Hosseini, J.M. Planeix, N. Kyritsakas. *New J. Chem.*, **5**, 683 (2006); (c) T.J. Burchell, D.J. Eisler, R.J. Puddephatt. *Inorg. Chem.*, **43**, 5550 (2004).
- [28] K. Uemura, S. Kitagawa, M. Kondo, K. Fukui, R. Kitaura, H.C. Chang, T. Mizutani. *Chem. Eur. J.*, **8**, 3586 (2002).
- [29] T.J. Burchell, D.J. Eisler, R.J. Puddephatt. *Inorg. Chem.*, **43**, 5550 (2004).
- [30] T.J. Burchell, D.J. Eisler, M.C. Jennings, R.J. Puddephatt. *Chem. Commun.*, 944 (2004).
- [31] B.L. Wu, L.Y. Meng, H.Y. Zhang, H.W. Hou. *J. Coord. Chem.*, **63**, 3155 (2010).
- [32] G.M. Sheldrick. *Acta Crystallogr., Sect. A: Found. Crystallogr.*, **64**, 112 (2008).
- [33] B.L. Wu, D.Q. Yuan, B.Y. Lou, L. Han, C.P. Liu, C.X. Zhang, M.C. Hong. *Inorg. Chem.*, **44**, 9175 (2005).
- [34] C.W. Cady, C. Incarvito, G.W. Brudvig, R.H. Crabtree. *Inorg. Chim. Acta*, **359**, 2509 (2006).
- [35] C.Y. Niu, B.L. Wu, X.S. Wan, H.Y. Zhang, H.Q. Zhang. *J. Mol. Struct.*, **973**, 194 (2010).